

Experimental testing of the variable rotated elastic parabolic equation

Harry J. Simpson^{a)}

Physical Acoustic Branch Code 7136, Naval Research Laboratory, 4555 Overlook Avenue, SW., Washington, D.C. 20375

Jon M. Collis

Department of Applied Mathematics and Statistics, Colorado School of Mines, 1500 Illinois Street, Golden, Colorado 80401

Raymond J. Soukup

Acoustics Division Code 7144, Naval Research Laboratory, 4555 Overlook Avenue, SW., Washington, D.C. 20375

Michael D. Collins

Naval Research Laboratory, Stennis Space Center, Mississippi 39529

William L. Siegmann

Department of Mathematical Science, Rensselaer Polytechnic Institute, 110 Eighth Street, Jonsson-Rowland Science Center 1C08, Troy, New York 12180

(Received 17 December 2010; revised 7 July 2011; accepted 28 August 2011)

A series of laboratory experiments was conducted to obtain high-quality data for acoustic propagation in shallow water waveguides with sloping elastic bottoms. Accurate modeling of transmission loss in these waveguides can be performed with the variable rotated parabolic equation method. Results from an earlier experiment with a flat or sloped slab of polyvinyl chloride (PVC) demonstrated the necessity of accounting for elasticity in the bottom and the ability of the model to produce benchmark-quality agreement with experimental data [J. M. Collis *et al.*, *J. Acoust. Soc. Am.* **122**, 1987–1993 (2007)]. This paper presents results of a second experiment, using two PVC slabs joined at an angle to create a waveguide with variable bottom slope. Acoustic transmissions over the 100–300 kHz band were received on synthetic horizontal arrays for two source positions. The PVC slabs were oriented to produce three different simulated waveguides: flat bottom followed by downslope, upslope followed by flat bottom, and upslope followed by downslope. Parabolic equation solutions for treating variable slopes are benchmarked against the data. [DOI: 10.1121/1.3641415]

PACS number(s): 43.30.Zk, 43.30.Ma [MS]

Pages: 2681–2686

I. INTRODUCTION

Acoustic properties of the ocean bottom usually have a significant effect on acoustic propagation in shallow water. The sediment can often be modeled as a fluid, but shear waves can be important when the bottom consists of exposed rock or a thin layer of sediment overlying a harder bottom. The interface between the ocean and sediment can be modeled as horizontal in some cases, but slope must be taken into account in many applications. When shear effects and range-dependence are both present, recent developments in the variable rotated parabolic equation method are required for accurate and efficient modeling. The variable rotated parabolic equation method is an effective approach for handling range-dependent problems,^{1,2} and the accuracy of this approach has been established for a limited set of seismo-acoustics problems through numerical and experimental benchmarking.^{3,4}

Spectral solutions are also being considered to treat these types of problems.^{5–9}

In this paper, results are presented from the second of a series of experiments designed to compare elastic variable rotated parabolic equation solutions with data from an experiment involving a slab of polyvinyl chloride (PVC) suspended in water. The first experiment (EPEE-1) featured two bottom configurations, flat and sloped, but did not involve slope changes.³ For the second experiment (EPEE-2), combinations of flat and sloping interfaces were considered that included a bottom slope change designed to simulate variable bathymetry. High-quality data were obtained using a robotic apparatus to move a receiver hydrophone to synthesize two-dimensional arrays. In order to handle sloping interfaces accurately, the variable rotated parabolic equation is used.^{10–12} As with the earlier experiment with PVC slabs, it is necessary to account for shear waves when making model comparisons.³ We were able to achieve good agreement by accurately inverting for geometric parameters (such as source depth and bathymetry), within the bounds of experimental uncertainty. Details of the experiment are

^{a)}Author to whom correspondence should be addressed. Electronic mail: harry.simpson@nrl.navy.mil

discussed in Sec. II. Comparisons with parabolic equation solutions are presented in Sec. III.

II. THE LABORATORY EXPERIMENT

The Elastic Parabolic Equation Experiment 2 (EPEE-2) was carried out in April 2007 in the Shallow Water Laboratory at the Naval Research Laboratory. The Shallow Water Laboratory contains a three-dimensional robotics system suspended over a 8 m wide by 11 m long by 4 m deep deionized water facility, with acoustic transmissions in the 100 to 300 kHz band. A range-dependent elastic bottom was modeled using two 122 cm \times 122 cm \times 10 cm slabs of PVC joined at a 5° angle. The slabs were suspended in water at different orientations by cables attached at the corners. An omni-directional source and receiver were placed in the

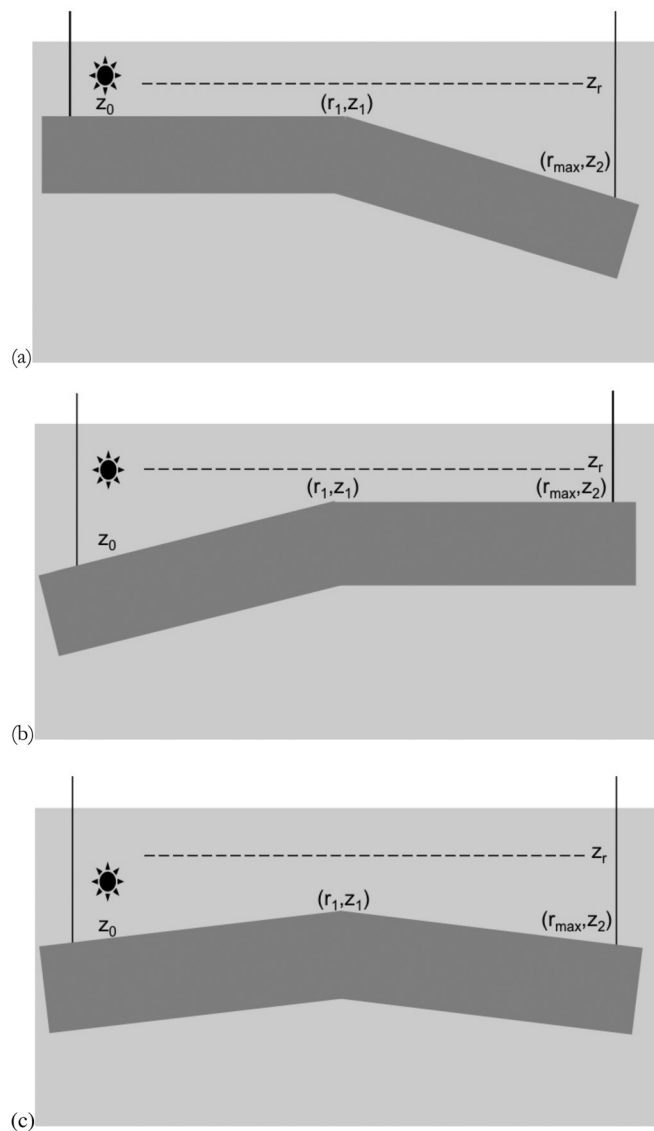


FIG. 1. Configuration of the laboratory experiment, including the dark gray-colored PVC slab, the cables attached near its corners, the large tank of deionized water, and the source and receiver positioning. A hundred transmissions were averaged for every combination of source and receiver position. (a) The flat to downslope case. (b) The upslope to flat case. (c) The upslope to downslope case.

waveguide using a robotic apparatus that allowed for accurate positioning and movement. The source was fixed while the receiver was moved in 2 mm increments away from the source. The slab, cables, source, and receiver are depicted in Fig. 1. Water temperature was maintained so that the sound speed remained within 1 m/s of 1482 m/s. Laboratory measurements of material samples in air¹³ provided estimates for the compressional and shear wave speeds (2290 and 1050 m/s) and the compressional and shear attenuations (0.76 and 1.05 dB/ λ) of the slab, which has a density of 1.378 g/cm³. The PVC material and hence geoaoustic parameters were chosen such that modeling of the slab would require inclusion of effects due to elasticity. The bottom is

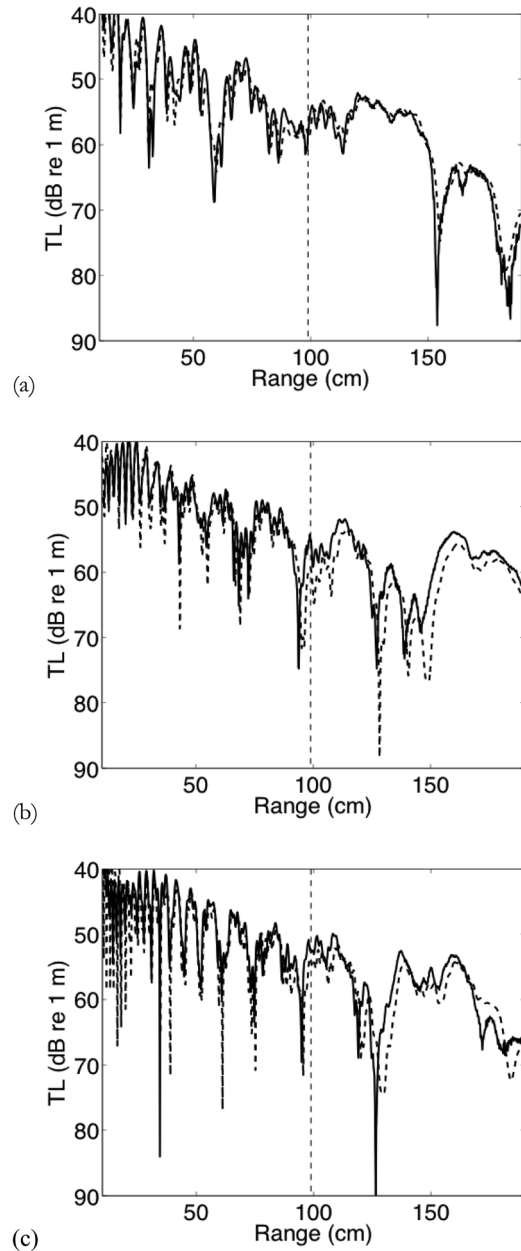


FIG. 2. Transmission loss versus range for the flat to downslope case, shallow source at 7.42 cm and deep receiver at 13.86 cm. Comparisons show data (solid curve) and calculations from the elastic parabolic equation (dashed curve), for source frequencies: (a) 125, (b) 200, and (c) 275 kHz. The dashed vertical line near 100 cm denotes the point of slope change in the bathymetry.

categorized as hard and could represent a granite (or other relatively dense solid) seafloor.

The transmitted waveform was an impulse with a flat frequency spectrum over the band 100–300 kHz. A reference measurement was made by positioning the source and receiver 1 m apart and measuring the pressure produced from a shaped pulse which was flat within the source band. Figure 2 in Ref. 3 shows the temporal and frequency responses for the reference measurement. Measurements were recorded at 8192 points with a 0.5 μ s sampling interval. Windowing was applied to eliminate reflections from the hardware and the walls of the tank. The windowed time series were Fourier transformed, resulting in 4096 data points that spanned 1 MHz in the frequency domain. A transfer function was obtained by multiplying the frequency response with the reciprocal of the spectrum of the reference pulse. Noise reduction was accomplished by averaging the received time series over the 100 transmissions for each source and receiver position.

Three cases involving propagation across a single change in slope are considered: flat to downslope, upslope to flat, and upslope to downslope. The propagation tracks were centered on the slab (in azimuth), with the source 100 cm in range from the change in slope and 22 cm beyond the rear edge of the slab. The receiver was moved horizontally between ranges of 10 and 190 cm from the source to produce a synthetic horizontal array. For each of the three cases, horizontal array data were collected for two source depths and two receiver depths at each source position. The slab had sufficient attenuation to prevent spurious reflections from its lower boundary (this was tested through modeling and during the first experiment). The geometrical parameters are the source depth z_s , receiver depth z_r , depth of the slab (water depth) directly below the source z_0 , depth of the slab at 100 cm (the range of the slope change) z_1 , and depth of the end the slab that is farthest from the source z_2 . These parameters were measured during the experiment, but there was sufficient uncertainty in their values to cause significant variability in model predictions of the highly

TABLE I. Inversion results for geometric parameters: flat to downslope case. The intended experimental geometry is given in the first column, followed by the values from a simulated annealing inversion.

Flat to downslope case	Nominal (measured)	Simulated annealing	Absolute error	Relative error (+/- %)
z_s mid (cm)	7.50	7.42	0.08	1.07
z_r mid (cm)	7.50	7.58	0.08	1.07
z_s mid (cm)	7.50	7.40	0.10	1.33
z_r deep (cm)	14.0	13.86	0.14	1.0
z_s deep (cm)	14.0	13.82	0.18	1.29
z_r mid (cm)	7.50	7.70	0.20	2.7
z_s deep (cm)	14.0	13.82	0.18	1.29
z_r deep (cm)	14.0	13.98	0.02	0.14
z_0 (@ $r = 0$)	15.0	14.39	0.61	4.07
r_1 (cm)	100.0	98.88	1.12	1.12
z_1 (@ r_1)	15.0	15.21	0.21	1.4
r_{\max} (cm)	190.0	189.31	0.69	0.36
z_2 (@ r_{\max})	22.87	23.82	0.95	4.15

TABLE II. Inversion results for geometric parameters: upslope to flat case. The intended experimental geometry is given in the first column, followed by the values from a simulated annealing inversion.

Upslope to flat case	Nominal (measured)	Simulated annealing	Absolute error	Relative error (+/- %)
z_s mid (cm)	7.50	7.35	0.15	2.0
z_r mid (cm)	7.50	7.87	0.37	4.93
z_s mid (cm)	7.50	7.33	0.17	2.27
z_r deep (cm)	14.0	14.02	0.02	1.43
z_s deep (cm)	14.0	13.71	0.29	2.07
z_r mid (cm)	7.50	7.83	0.33	4.4
z_s deep (cm)	14.0	13.82	0.18	1.29
z_r deep (cm)	14.0	14.15	0.15	1.07
z_0 (@ $r = 0$)	24.45	24.59	0.14	4.07
r_1 (cm)	100.0	98.59	1.41	1.41
z_1 (@ r_1)	15.0	15.12	0.12	0.8
r_{\max} (cm)	190.0	189.45	0.55	0.29
z_2 (@ r_{\max})	15.0	14.57	0.43	2.87

structured transmission loss curves. The sources of uncertainty in these parameters include the finite sizes of the transducers and slight irregularities in the surface of the slab. In order to optimize the agreement between data and model, we applied simple inversion techniques to derive corrections to the measured values. The measured and inverted values are given in Tables I, II, and III for the three cases. Note that for the first two cases, the slab configuration was fixed in the water and the source and receivers were interchanged to produce the different cases; inverted bottom depth values are the same for both cases.

III. COMPARISON WITH PARABOLIC EQUATION SOLUTIONS

In this section, comparisons are presented between the laboratory data and rotated elastic parabolic equation at the select frequencies of 125, 200, and 275 kHz. Results presented at these frequencies are representative of those obtained at other frequencies within the frequency band of

TABLE III. Inversion results for geometric parameters: upslope to downslope case. The intended experimental geometry is given in the first column, followed by the values from a simulated annealing inversion.

Upslope to downslope case	Nominal (measured)	Simulated annealing	Absolute error	Relative error (+/- %)
z_s mid (cm)	7.50	7.21	0.29	3.87
z_r mid (cm)	7.50	7.48	0.02	0.27
z_s mid (cm)	7.50	7.12	0.38	5.07
z_r deep (cm)	14.0	13.63	0.37	2.64
z_s deep (cm)	14.0	13.65	0.35	2.5
z_r mid (cm)	7.50	7.64	0.14	1.87
z_s deep (cm)	14.0	13.69	0.31	2.21
z_r deep (cm)	14.0	13.83	0.17	1.21
z_0 (@ $r = 0$)	19.37	18.30	1.07	5.52
r_1 (cm)	100.0	100.03	0.03	0.03
z_1 (@ r_1)	15.0	14.98	0.02	0.13
r_{\max} (cm)	190.0	189.50	0.50	0.26
z_2 (@ r_{\max})	18.93	19.89	0.96	5.07

the source signal. Data comparisons were made using the variable rotated elastic parabolic equation.^{11,12} The solution uses an improved formulation of elasticity,² has been benchmarked against other elastic parabolic equations,¹¹ and is currently viewed to be the most accurate elastic parabolic equation implementation. The solution is implemented in FORTRAN 77 and runs on any modern computer without special hardware considerations. Note that the model is scaled 1000:1 in length, which means that simulations are computed at 125, 200, and 275 Hz.

For the flat to downslope case, the source was placed at two different depths to excite different combinations of modes. The bottom slope is approximately 5°. The receiver

is near the bottom of the water column for the two source positions. Appearing in Fig. 2 are results for the case of the source near the middle of the water column. The elastic parabolic equation solutions are in excellent agreement with the data prior to the slope change at 100 cm. Beyond the slope change, the pattern phase of the two solutions disagree and the resulting error increases with frequency. Appearing in Fig. 3 are results for the case of the source near the bottom of the water column, which causes the higher modes to be relatively highly excited. The elastic parabolic equation solutions appearing in Fig. 3 are in good agreement with the data for all three frequencies, but there are some errors over the downslope portion of the slab.

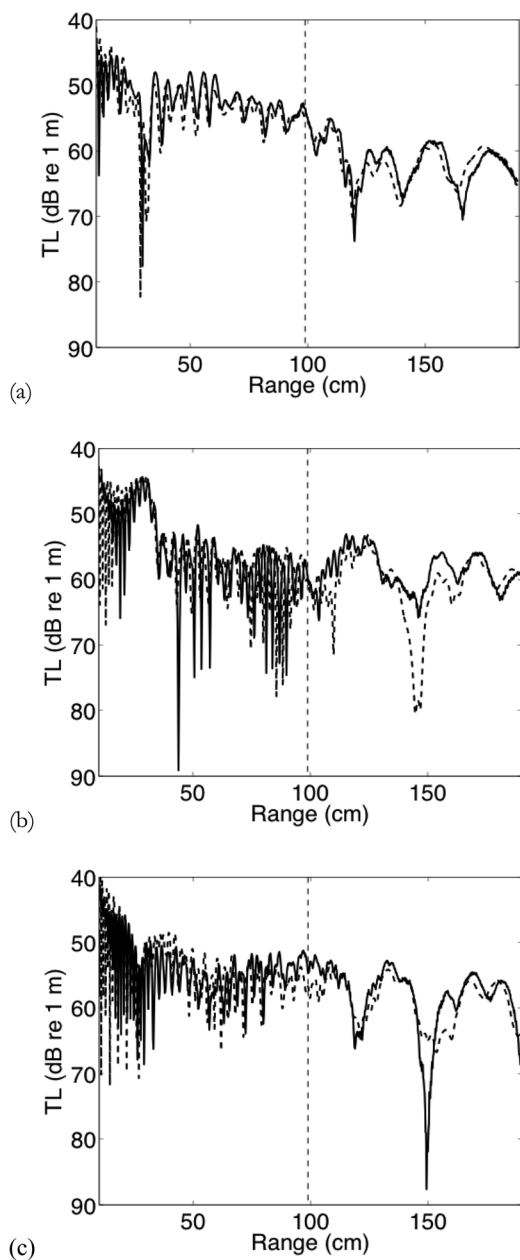


FIG. 3. Transmission loss versus range for the flat to downslope case, deep source at 13.82 cm and deep receiver at 13.98 cm. Comparisons show data (solid curve) and calculations from the elastic parabolic equation (dashed curve), for source frequencies: (a) 125, (b) 200, and (c) 275 kHz. The dashed vertical line near 100 cm denotes the point of slope change in the bathymetry.

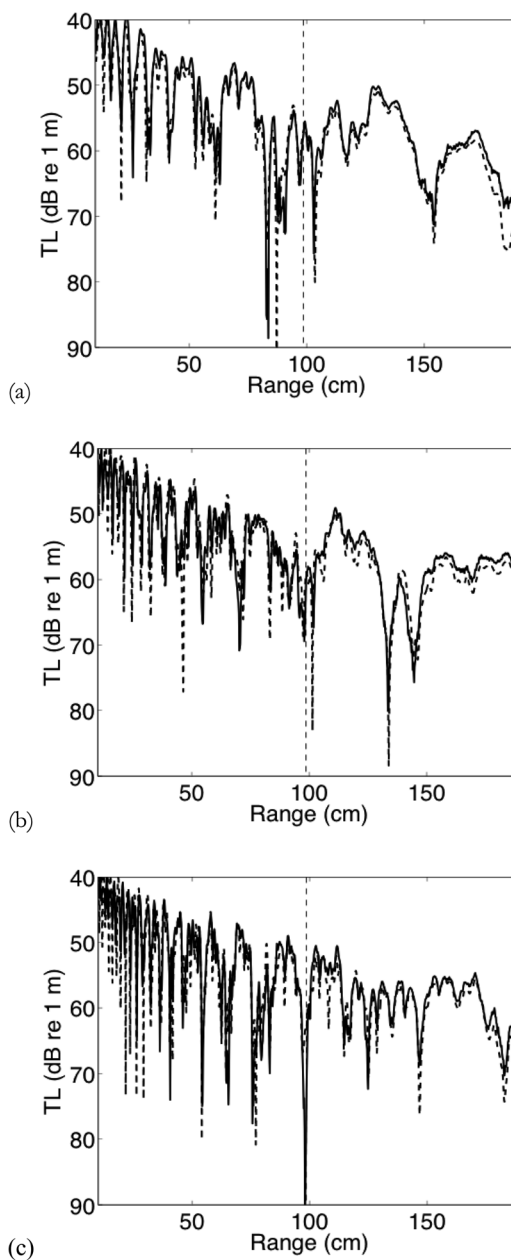


FIG. 4. Transmission loss versus range for the upslope to flat case, deep source at 13.71 cm and shallow receiver at 7.83 cm. Comparisons show data (solid curve) and calculations from the elastic parabolic equation (dashed curve), for source frequencies: (a) 125, (b) 200, and (c) 275 kHz. The dashed vertical line near 100 cm denotes the point of slope change in the bathymetry.

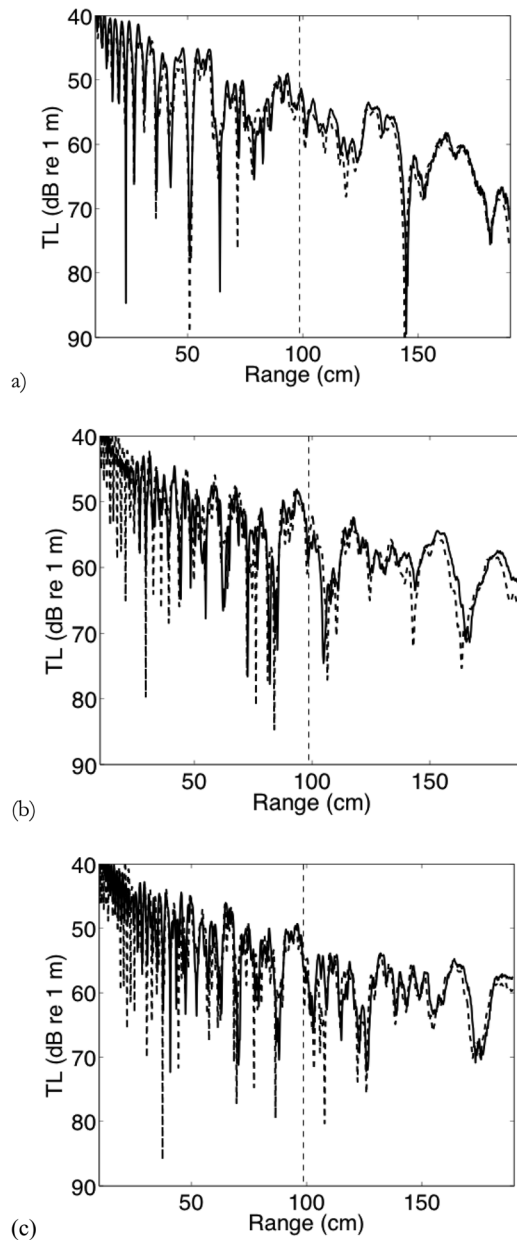


FIG. 5. Transmission loss versus range for the upslope to flat case, deep source at 13.82 cm and deep receiver at 14.15 cm. Comparisons show data (solid curve) and calculations from the elastic parabolic equation (dashed curve), for source frequencies: (a) 125, (b) 200, and (c) 275 kHz. The dashed vertical line near 100 cm denotes the point of slope change in the bathymetry.

For the upslope to flat case, two positions are considered for the receiver depth, and the source near the bottom of the water column for both receiver positions. The slab was kept in the same position, and the changes in slope were created by interchanging source and receiver positions. Appearing in Fig. 4 are results for the case of the receiver near the middle of the water column. The elastic parabolic equation solutions are in excellent agreement with the data. Appearing in Fig. 5 are results for the case of the receiver near the bottom of the water column. The elastic parabolic equation solutions in Fig. 5 are in good agreement with the data for all three frequencies.

For the fully range-dependent case, the bottom slope transitions from approximately 1.9° upslope to 3.1° down-

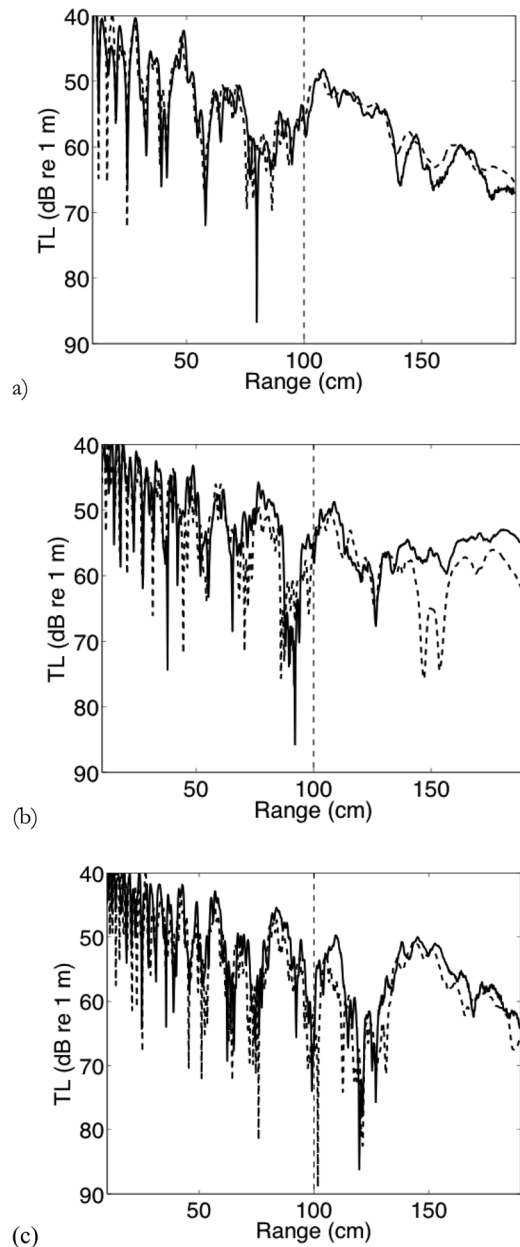


FIG. 6. Transmission loss versus range for the upslope to downslope case, deep source at 13.65 cm and shallow receiver at 7.64 cm. Comparisons show data (solid curve) and calculations from the elastic parabolic equation (dashed curve), for source frequencies: (a) 125, (b) 200, and (c) 275 kHz. The dashed vertical line near 100 cm denotes the point of slope change in the bathymetry.

slope. Results for the case of a deep source and shallow receiver appear in Fig. 6. As with the other cases, there is excellent agreement between the elastic parabolic equation solution and the data over the upsloping bottom, but amplitude differences are evident over the downsloping bottom. An extensive set of additional cases were considered for other frequencies and source and receiver positions and obtained similar results for each case.

IV. CONCLUSIONS

Results have been presented for a scale-model underwater acoustic laboratory experiment that featured acoustic

propagation over a penetrable elastic slab. The bathymetry, represented by the slab, was designed such that it was range-dependent for part of or the entire propagation track. Measurements were conducted for three cases: upslope to range-independent propagation, range-independent to downslope propagation, and range-dependent propagation up to and beyond a ridge. In each of the cases, the change in slope was approximately 5° . The experimental data has been compared against elastic parabolic equation solution calculations that employ coordinate transformation techniques to handle range-dependent bathymetry. Agreement between simulated and measured data is excellent in each of the cases. An initial conclusion from this work is that coordinate rotations are an effective and accurate technique for treating range-dependent bathymetry. Additionally, the comparisons established in this work verify that the parabolic approximation is accurate and is fully capable of modeling range-dependent propagation for ocean bottom slopes of up to 5.0° . That is, in these cases backscatter is significantly small as to be negligible for environments with this bottom slope.

Of the three propagation scenarios considered in this work, agreement was best for the upslope to range-independent propagation case. In the upslope case, differences between simulation and measurement remained constant over the range of the comparison track, with no noticeable change in character beyond the point of slope change. For the range-independent to downslope propagation case, differences between measurement and simulation are greater beyond the point of slope change. This case that involves downslope propagation is the more difficult to model due to evanescent wave field coupling to the propagating wave field beyond the point of slope change. Although errors are greater beyond the point of slope change, the calculated solution accurately captures both the amplitude and pattern phase of the field. Differences for the fully range-dependent case are similarly explained.

Results from this second in a series of laboratory experiments strongly support those of the first: Excellent agreement has been obtained between elastic parabolic equation solutions and data from a laboratory experiment for range-dependent seismo-acoustic propagation problems involving variable bathymetry. The details of the highly structured transmission loss curves line up well in comparisons. The results indicate that the laboratory data are of high quality

and that the parabolic equation solutions are accurate. To obtain high-quality agreement for data comparisons, it was necessary to apply inverse techniques to refine the values of geometric parameters that were measured during the experiment.

ACKNOWLEDGMENTS

This work was supported by the Office of Naval Research. J.M.C. was partially supported by an ONR Ocean Acoustics Postdoctoral Fellowship Grant.

- ¹M. D. Collins, "Higher-order Padé approximations for accurate and stable elastic parabolic equations with application to interface wave propagation," *J. Acoust. Soc. Am.* **89**, 1050–1057 (1991).
- ²W. Jerzak, W. L. Siegmann, and M. D. Collins, "Modeling Rayleigh and Stonely waves and other interface and boundary effects with the parabolic equation," *J. Acoust. Soc. Am.* **117**, 3497–3503 (2005).
- ³J. M. Collis, W. L. Siegmann, M. D. Collins, H. J. Simpson, and R. J. Soukup, "Comparison of simulations and data from a seismo-acoustic tank experiment," *J. Acoust. Soc. Am.* **122**, 1987–1993 (2007).
- ⁴J. M. Collis, W. L. Siegmann, F. B. Jensen, M. Zampolli, E. T. Kusel, and M. D. Collins, "Parabolic equation solution of seismo-acoustics problems involving variations in bathymetry and sediment thickness," *J. Acoust. Soc. Am.* **123**, 51–55 (2008).
- ⁵J. T. Goh, H. Schmidt, P. Gerstoft, and W. Seong, "Benchmarks for validating range-dependent seismo-acoustic propagation codes," *IEEE J. Ocean. Eng.* **22**, 226–236 (1997).
- ⁶I. T. Lu and L. B. Felsen, "Adiabatic transforms for spectral analysis and synthesis of weakly range-dependent shallow ocean Green's functions," *J. Acoust. Soc. Am.* **81**, 897–911 (1987).
- ⁷J. T. Goh and H. Schmidt, "Validity of spectral theories for weakly range-dependent ocean environments—numerical results," *J. Acoust. Soc. Am.* **95**, 727–732 (1994).
- ⁸H. Schmidt, W. Seong, and J. T. Goh, "Spectral super-element approach to range-dependent ocean acoustic modeling," *J. Acoust. Soc. Am.* **98**, 465–472 (1995).
- ⁹J. T. Goh and H. Schmidt, "A hybrid coupled wavenumber integration approach to range-dependent ocean acoustic modeling," *J. Acoust. Soc. Am.* **100**, 1409–1420 (1996).
- ¹⁰M. D. Collins, "The rotated parabolic equation and sloping ocean bottoms," *J. Acoust. Soc. Am.* **87**, 1035–1037 (1990).
- ¹¹D. A. Outing, W. L. Siegmann, M. D. Collins, and E. K. Westwood, "A rotated parabolic equation for variable slopes," *J. Acoust. Soc. Am.* **120**, 3534–3538 (2006).
- ¹²J. M. Collis, W. L. Siegmann, M. Zampolli, and M. D. Collins, "Extension of the rotated elastic parabolic equation to beach and island propagation," *J. Ocean. Eng.* **34**, 617–623 (2009).
- ¹³R. J. Soukup, H. J. Simpson, E. C. Porse, J. E. Summers, and R. F. Gragg "Geoacoustic physical modeling elastic parabolic equation 1 (GPM EPE1) experiment: Measurement report and acoustic data," Naval Research Laboratory Memorandum, Report No. 7140-04-8826 (2004).